The Servo System for Antenna Positioning

By J. C. LOZIER, J. A. NORTON, and M. IWAMA

(Manuscript received January 22, 1963)

This paper describes the servo system for pointing the horn-reflector antenna. It presents the general considerations which dictated the design and also describes the resulting system in some detail, giving the characteristics of the various parts of the system. Finally, the over-all performance of the servo system is discussed.

I. INTRODUCTION

The needs of broadband satellite communications systems for a high-gain, low-noise antenna led to the choice of the horn type structure. High gain and low noise inherently mean a narrow-beam antenna and, therefore, an antenna with a large reflector which has to be pointed very accurately. In this case, the beamwidth is such that at 4 kmc, the strength of the received signal is 3 db down when the antenna is pointed 0.11° off center. However, in order to conserve signal-to-noise ratio, maximum reduction in received signal strength of 1 db was alloted to errors in pointing.[1] This places an over-all accuracy requirement of 0.06 degree maximum error on the antenna pointing system.

The dynamic requirements on the control system are generated by the orbits of the satellites to be tracked and by the nature of the antenna mount. With an azimuth-elevation mount, it takes a very high azimuth velocity to track a low-altitude satellite passing close to the zenith, and a very low azimuth velocity to track a satellite pass as it comes up over the horizon. The compromise objective set for the system was that it be able to track smoothly and accurately all satellite passes with maximum azimuth velocities up to 0.5 degree per second. For a satellite with a 2500-mile altitude, typical of the first Telstar satellite orbits, the 0.5 degree per second velocity would limit the tracking to passes having maximum angle of elevation less than 81 degrees. However, for satellites with altitudes of 6000 miles and above, the maximum trackable angles of elevation would be 86°.

Two methods of pointing the antenna at the satellite were considered. In one method, the antenna is driven by pointing information derived in advance from the predicted path of the satellite.[2] This is called the "program command" mode. In this mode, pointing information from the digital part of the antenna control system[3] is compared with the encoded outputs of position pick-offs on the mechanical axes to derive the actuating signals for the antenna drive. This mode of operation is subject to errors in prediction and in the calibration of the electrical vs mechanical axes of the antenna, as well as servo errors. A maximum of $\pm 0.2°$ of the total maximum 0.06° error was allocated to the servo in this mode; this amounts to 0.014° in each axis.

In another method, the antenna is driven by pointing information provided by an autotrack system.[4] In this autotrack mode, the autotrack system generates tracking error signals from a microwave beacon on the satellite, and these signals are used for aligning the electrical axes of the horn antenna with the satellite. The autotrack mode is not subject to the errors of orbital prediction or antenna calibration inherent in the program command mode. However, initial pointing information aid is required, because the acquisition range of the autotrack system is only $\pm 0.02°$ about the satellite position.

Since the system is experimental and the two methods are compatible, provisions are made so that either of these methods alone or a combination of the two can be used to control antenna pointing. When the two modes are combined, tape commands are used to place the antenna beam on the satellite, and the autotrack is used as a vernier to center the beam precisely. This tracking mode, called the "combined mode," unites the accuracy of the autotrack mode with the acquisition capabilities of the program command mode.

II. GENERAL DESIGN CONSIDERATIONS

For a satellite in a circular orbit with a maximum azimuth velocity of 0.5°/sec, the maximum azimuth acceleration is 0.003°/sec^2. These maxima define the input signal spectrum that the azimuth axis must follow in tracking a satellite. The spectrum and accuracy requirements determine the open-loop gain and phase requirements for azimuth. A system using two integrations was selected in order to meet the open loop gain requirement. This resulted in the open-loop gain vs frequency characteristic shown in Fig. 1. Shaping near the gain crossover frequency is necessary for stability reasons. To track with a maximum acceleration of 0.003°/sec^2 with an accuracy of 0.014° means that the gain crossover

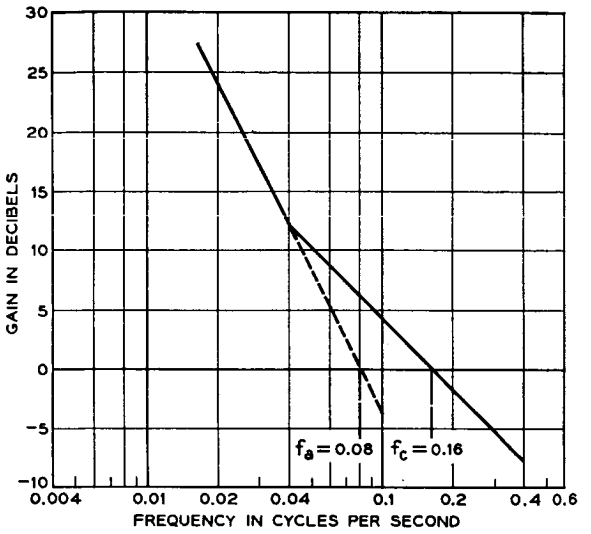

Fig. 1 — Open-loop gain vs frequency characteristic meeting system design objectives.

frequency (f_a) of the projected −12 db per octave asymptote must be at least 0.08 cps, as shown in Fig. 1. In order to realize this frequency with adequate phase margin, the lowest resonant frequency of the combined antenna and drive system must be over 0.64 cps.

Since the antenna and control system were designed and built at one time, it was not clear that the above requirements could be met. Therefore the program command mode was designed to provide and utilize velocity as well as position commands. Velocity command would have been needed if the servo bandwidth could not have been made large enough. However, this proved to be unnecessary, since the primary structural resonance in azimuth was found to be 1.8 cps.[5] Furthermore, the low Q of the antenna structure plus damping at the resonant frequency provided by a pressure feedback loop around the hydraulic motor drives resulted in an effective Q for the system of approximately 3. As a result, an open-loop gain vs frequency characteristic having a gain crossover frequency f_c of 0.4 cps has been achieved, as shown in Fig. 13 of Section 4.1. This gave the ability to track satisfactorily any satellite pass up to the maximum antenna velocity in azimuth of 1.5°/sec.

Other design considerations arise from the need to track accurately at very low speeds. The antenna is supported on rails by four two-

wheeled trucks[5] which develop large discontinuous torques about the azimuth axis at very low turning velocities. Accurate tracking at these speeds requires minimization of the system response to these torques. A peak response of less than 0.014° for a step change of 50,000 ft-lbs applied to the azimuth turntable was the design objective. System responses to these torques are determined by the position feedback loop, antenna inertia, and drive system stiffness. The position feedback loop increases system stiffness at low frequencies; the two integrations in the loop reduce the error due to a constant friction torque to essentially zero. The inertia of the antenna is effective in minimizing the response of the system to the disturbance torques at high frequencies. Hydraulic motor drives were chosen because of their high stiffness, large bandwidth and high acceleration capability. The drive stiffness was further increased by the use of velocity feedback. Compliance of the 15,107:1 gear reduction in azimuth was minimized by the use of a 64-ft diameter bull gear mounted on the antenna foundation and driven by large gear boxes mounted rigidly to the azimuth turntable. The effect of backlash in the gear trains was eliminated by the use in each drive of two opposing hydraulic motors coupled to the bull gear through individual gear trains. As a result of these precautions, a step change in torque of 200,000 ft-lbs rather than 50,000 ft-lbs is required to get a peak error response of 0.014°.

On account of the very large torques that high wind velocities could exert on the horn structure (10^6 ft-lbs at 30 mph), it was clear very early in the project that a radome would be required if the system was to operate reliably under all weather conditions.[5]

Because of the complexity of the servo system and the various nonlinearities present, analog computer simulations have been used extensively for the synthesis and analysis of the proposed configurations. As one of the significant results obtained from the analog computer studies, it was learned that a pressure feedback loop from hydraulic transmissions is not only effective, but essential, for damping out the oscillatory motion of the antenna. The simulations also provided a convenient means for determining the gains of the various minor feedback loops and their effects on the over-all performance. Completely analytical approach would not have been practical because of small as well as large signal nonlinearities present. The final modifications and adjustments of the gains were made on the basis of performance of the actual antenna servo.

III. DRIVE SYSTEM

This section describes the hydraulic transmissions and the associated minor feedback loops, including yoke position, pressure difference, pres-

sure and velocity loops. A functional diagram of the over-all drive system is shown in Fig. 2.

1.3 *Hydraulic Transmission*

Each hydraulic drive system contains a pair of hydraulic transmissions.[5] Each hydraulic transmission is composed of one constant-speed, variable-displacement pump and a pair of constant-displacement motors with output pinions connected to the bull gear through individual gear trains. Pump displacement is controlled by the yoke position.

The two hydraulic transmissions used in the azimuth axis are rated at 25 HP each, and those used in the elevation axis are rated at 10 HP each. The 25-HP unit is capable of developing a maximum output torque of 38 ft-lbs, while a 10-HP unit is capable of delivering 15 ft-lbs. These values correspond to 0.55×10^6 ft-lbs and 0.27×10^6 ft-lbs of torque, respectively, at the bull gear. The actual torques available at the bull gears are reduced by about 10 per cent in overcoming the friction torques. The gear ratios are 15,107:1 for the azimuth axis and 18,344:1 for the elevation axis. Since the inertias (including those of the motors and gear trains) for the two axes are 41×10^6 slug-ft^2 for azimuth and 7.4×10^6 slug-ft^2 for elevation, the maximum accelerations attainable are 1.3 degrees per second squared for the azimuth and 3.0 degrees per second squared for the elevation. The maximum motor velocity is 4200 rpm for both axes. The maximum antenna velocities are 1.5 degrees per second for the azimuth and 1.4 degrees per second for the elevation.

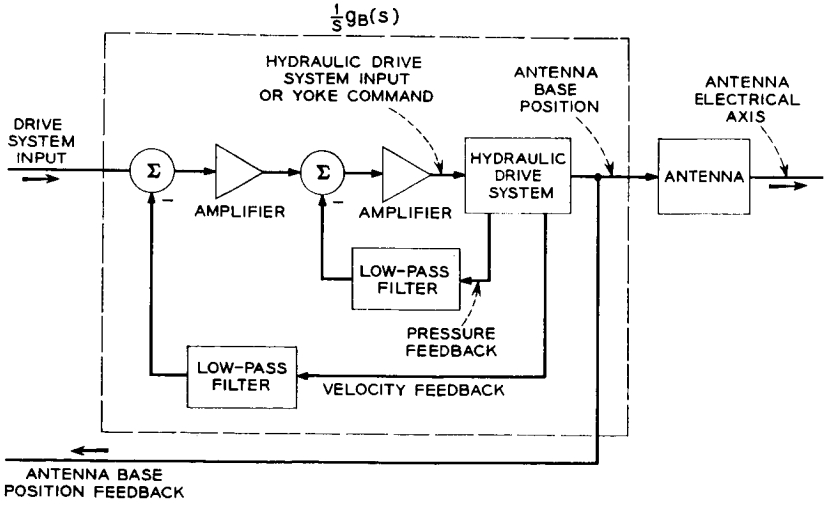

Fig. 2 — Functional diagram of drive system.

A linearized differential equation of the 25-HP unit is:

$$K_L P + K_C(dp/dt) + (d\theta_M/dt) = K_Y Y$$

where

$K_L = 4 \times 10^{-3}$ (radians/second)/(psi)
$K_C = 3.7 \times 10^{-3}$ (radians/second)/(psi/second)
$K_Y = 15$ (radians/second)/(degrees).

Here, Y is the yoke position in degrees, P is the pump pressure in psi, and θ_M is the motor pinion position in radians. The saturation values of Y and P are 30 degrees and 2200 psi respectively. The conversion factor from the pressure to torque is 0.017 ft-lb per psi.

The torque required to overcome friction in the system is a highly nonlinear function of the velocity. This is illustrated in Fig. 3, which shows the average torque required to drive the azimuth axis as a function of velocity.

The friction characteristics in the elevation axis are similar.

This discontinuity of the torque required to overcome friction around zero velocity produces a corresponding nonlinearity in the antenna velocity versus yoke position characteristic shown in Fig. 4. Since the slope of antenna velocity versus yoke position is a measure of the effective gain in the drive system, the small signal gain is highly nonlinear when the average velocity is low.

The hydraulic transmission also has large signal nonlinearities due to such factors as the velocity and amplitude limitations on the motion of the hydraulic yoke, and the hydraulic pressure limitations on the drive motors. However, these large signal nonlinearities are not as difficult to handle as the small signal nonlinearities discussed above.

3.2 *Yoke Position Loop*

The yoke position loop is the innermost of the minor feedback loops in the drive system, as shown on Fig. 5. As the name implies, this loop is designed to control the position of the pump yoke, which in turn controls the motor velocity.

The yoke mechanism is subject to both velocity and position limitations. Position limiting decreases the loop gain but does not degrade the phase characteristics. However, velocity limiting does introduce an additional phase lag which can be as large as 90 degrees. The closed-loop gain versus frequency response characteristics for three different input

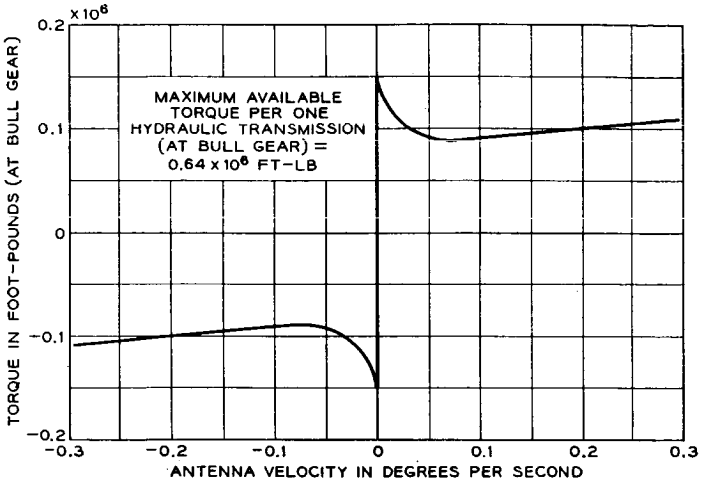

Fig. 3 — Average friction torque at constant velocity — azimuth.

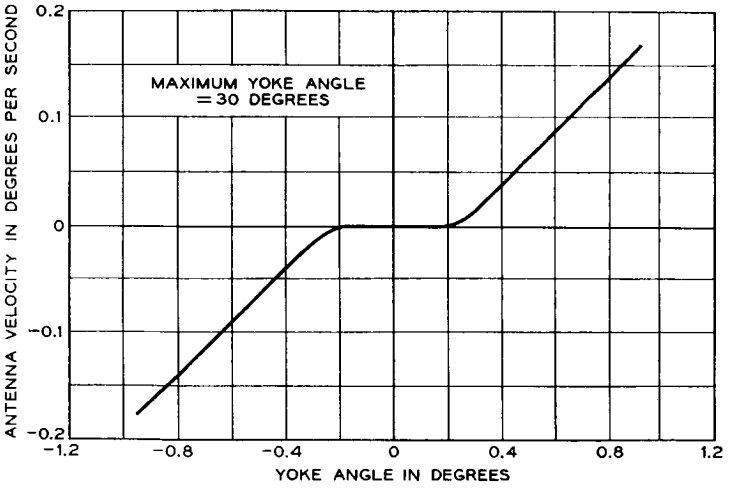

Fig. 4 — Antenna velocity vs yoke position characteristic for one hydraulic transmission — azimuth.

levels are shown on Fig. 6 to illustrate the degradation of the phase characteristic with load.

Allowance was made in designing the rest of the hydraulic drive system for this additional phase shift, so that the system is absolutely stable for large signals.

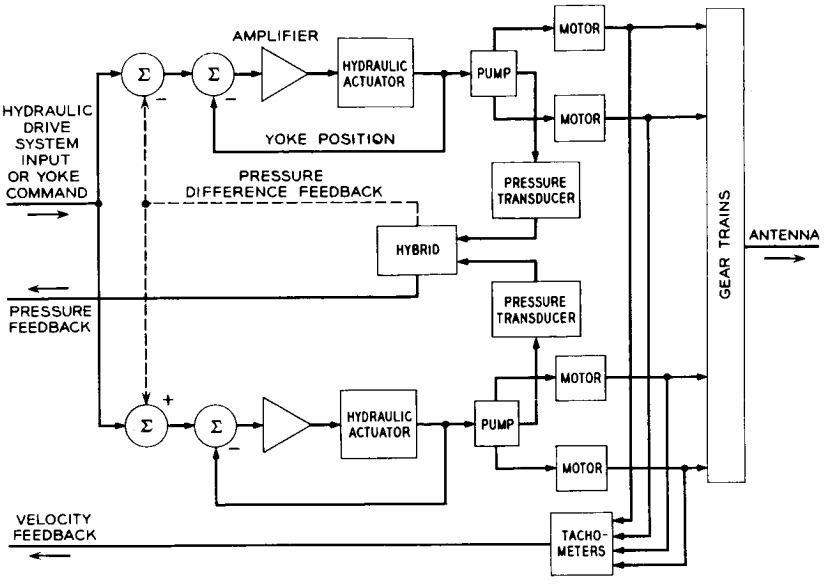

Fig. 5 — Functional diagram of hydraulic drive system.

3.3 *Pressure Difference Loop*

Since two hydraulic transmissions are used per axis to position the antenna, some means for equalizing the load on the two units is necessary. The pressure difference loop performs this function. A voltage proportional to the pressure difference is developed and fed back so as to reduce the yoke position of one unit and increase the other. In this way, the pressures, and consequently the output torques of the two transmissions, are equalized. The pressure difference loop is shown in dashed lines in Fig. 5.

3.4 *Pressure Loop*

It is the function of the pressure feedback loop to minimize the effects of the primary resonance of the combined antenna structure and hydraulic drive system, and this is accomplished by damping the system near its resonant frequency.

The way that the pressure feedback provides damping is easily shown on the electrical analog of the drive system presented in Fig. 7. The equivalent circuit of the antenna is derived from a simplified two-mass-

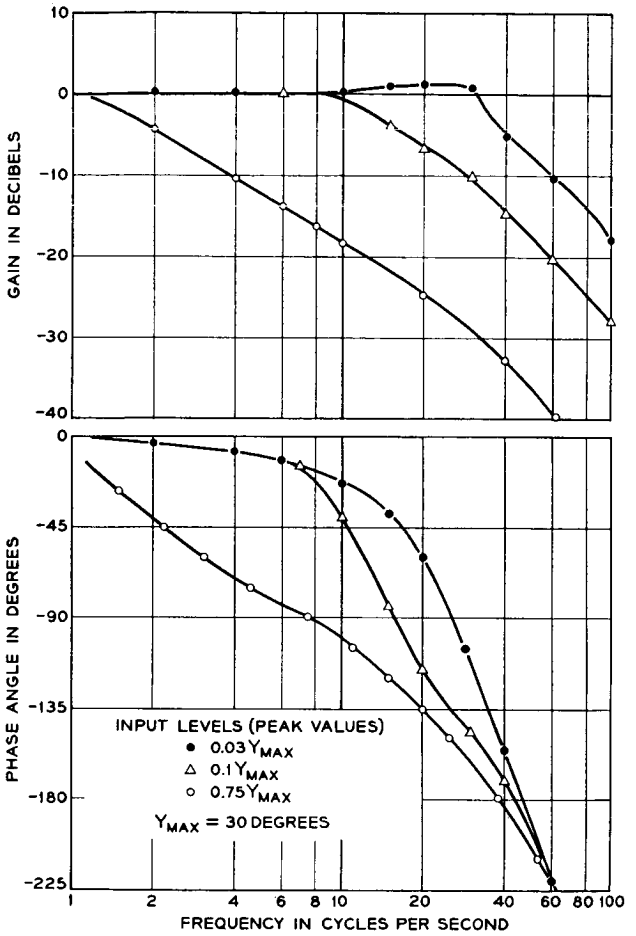

Fig. 6 — Closed-loop frequency response of yoke position — azimuth.

and-spring model, but this simplification does not affect the discussion here. The important point here is that the application of pressure feedback to the system is equivalent to adding a resistance, R_P, in the first mesh of the equivalent circuit. R_P is proportional to the gain of the pressure feedback loop.

It is clear that at resonance the equivalent circuit presents a low impedance to the driving voltage e_Y. R_P will be most effective in reducing the driving current i_M that can flow in the network at resonance

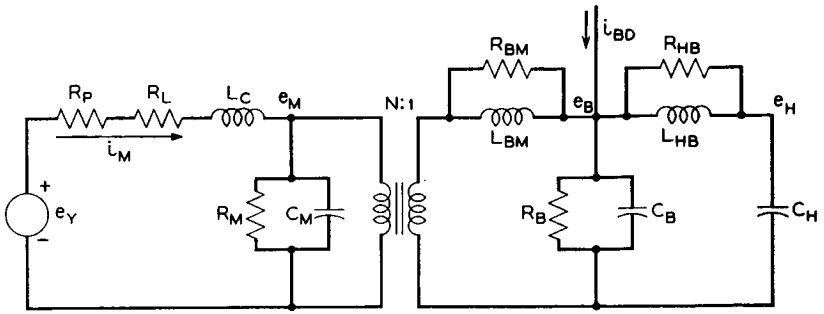

RELATION BETWEEN ORIGINAL AND ANALOGUE QUANTITIES

ELECTRICAL	MECHANICAL
e_Y	YOKE ANGLE
e_M, e_B, AND e_H	VELOCITIES OF MOTOR, ANTENNA BASE, ANTENNA HORN OR ELECTRICAL AXIS
i_M	HYDRAULIC TORQUE
i_{BD}	TORQUE DISTURBANCE AT BASE
R_L AND L_C	HYDRAULIC TRANSMISSION LEAKAGE AND COMPLIANCE
C_M, C_B AND C_H	INERTIAS OF MOTOR, ANTENNA BASE, AND ANTENNA HORN
L_{BM} AND L_{HB}	COMPLIANCES
R_M, R_{BM}, R_B, AND R_{HB}	MECHANICAL FRICTIONS
N	GEAR RATIO
R_P	EFFECT OF PRESSURE FEEDBACK

Fig. 7 — Electrical analog of hydraulic drive system and antenna.

when the impedance of the load is low. In addition to this, R_P helps to damp out transients that might be set up in the system by the torque disturbance, i_{BD} .

Thus the pressure feedback reduces the driving torques that the hydraulic drive system can deliver to the antenna structure at resonance, and it also helps to damp out transients set up in the system by disturbance torques.

The increase in the driving impedance that the antenna sees as a result of pressure feedback reduces the effective stiffness of the driving system. However, the driving system with pressure feedback allows

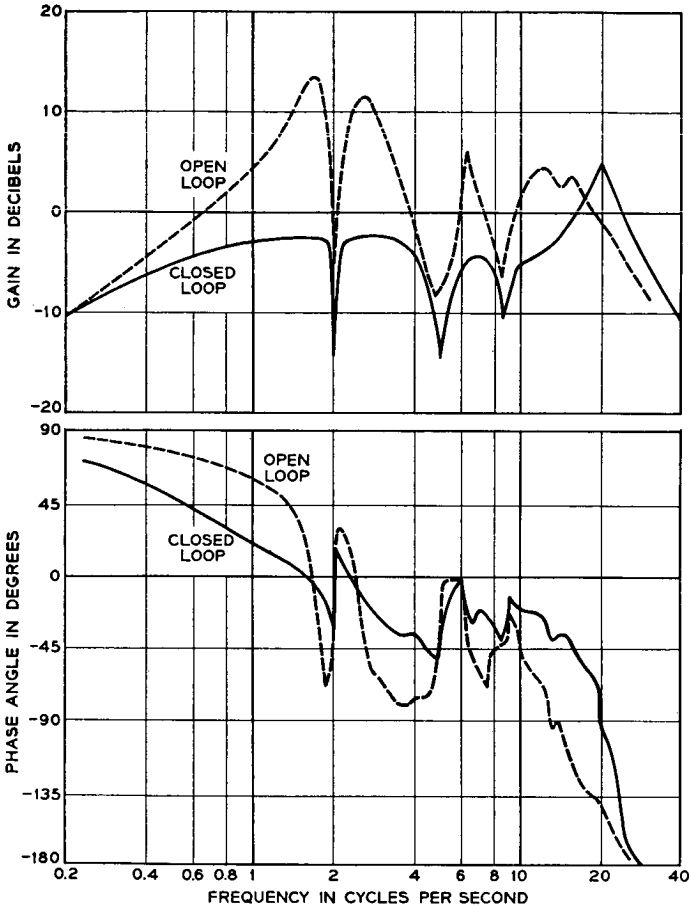

Fig. 8 — Open- and closed-loop frequency response of hydraulic pressure — azimuth.

higher gains in the velocity and position feedback loops at frequencies below resonance so that the effective hydraulic drive system stiffness is maintained at lower frequencies. It is important to keep the hydraulic drive system as stiff as possible to minimize the effects of friction at very low tracking velocities.

The effects of the pressure feedback loop on the characteristics of the combined antenna and hydraulic drive system are shown in Figs. 8 and 9. Here, the input is the driving voltage applied to the hydraulic drive

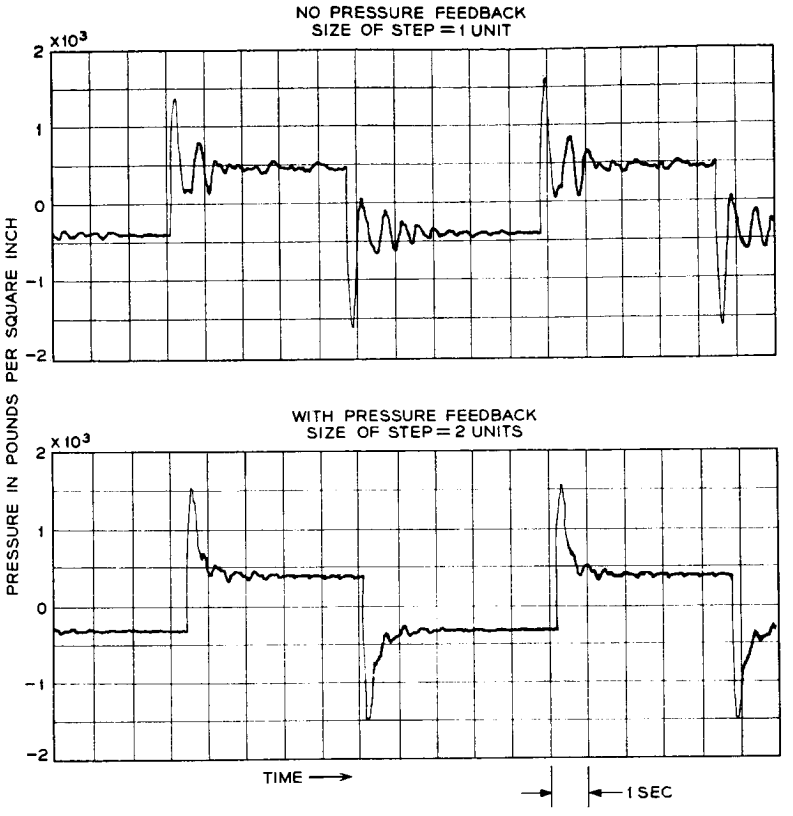

Fig. 9 — Pressure response to a step input with and without pressure feedback — azimuth.

system, and the gain is defined as the ratio of the pressure transducer output to the driving voltage. The gain versus frequency characteristics show that the closing of the pressure loop lowers the driving torque some 16 db at 1.8 cps where the combined antenna and drive system has its primary resonance. The pressure feedback also serves to suppress other resonances in the system all the way out to 15 cps. These curves also show that as far as the gains of the other loops are concerned, the effect of the pressure feedback is negligible at 0.2 cps and below. It should be noted also that the pressure feedback improves the phase versus frequency characteristics at 1 cps. This permits the use of a high-velocity loop gain and ultimately serves to improve the bandwidth and stability of the entire tracking system.

The damping effect is clearly illustrated in the step responses shown in Fig. 9. It is worth noting that two different input step sizes are used, although the peaks in the transient response with and without feedback are comparable in magnitude. It is apparent that the oscillations in pressure are greatly reduced by the use of the pressure feedback. The steady state pressure is equal to the pressure required to overcome the friction torque.

3.5 *Velocity Loop*

The outermost of the minor feedback loops is the velocity feedback loop. Velocity feedback is effectively shunt feedback, and it lowers the impedance of the driving system, in contrast to the effect of pressure feedback discussed above. Its primary function is consequently to increase the stiffness of the driving system at low frequencies. This is important in minimizing the effects of torque disturbances on the system. The other function of the velocity feedback loop is to reduce the system sensitivity to changes in leakage and compliance of the hydraulic transmissions.

The open- and closed-loop frequency characteristics presented on Fig. 10 show how velocity feedback improves the phase and gain characteristics at frequencies below the primary resonance. The improvement in phase margin in the frequency range between 0.2 and 0.8 cps, where the over-all position control loop will have its gain crossover, is as much as 32°. The reduction in gain is 7 db or more at 0.4 cps and below, thereby increasing the effective stiffness of the system to torque disturbances by some 2 to 1 in this critical frequency range. A low-pass network cuts the high-frequency gain of the velocity loop and makes the effect of velocity feedback negligible at higher frequencies.

The hydraulic drive system with all the minor feedback loops closed will be referred to simply as "the drive system" in subsequent sections. A functional diagram of the drive system is shown in Fig. 2. The transfer function $(1/s)g_B(s)$ relates the antenna base position to the drive input system.

IV. ANTENNA POSITION CONTROLS

Two different methods of pointing the antenna at the satellite are incorporated in the system. From the servo standpoint this means that there are two different ways of deriving error signals for closing the position control loop. One way is to use position pick-offs on the me-

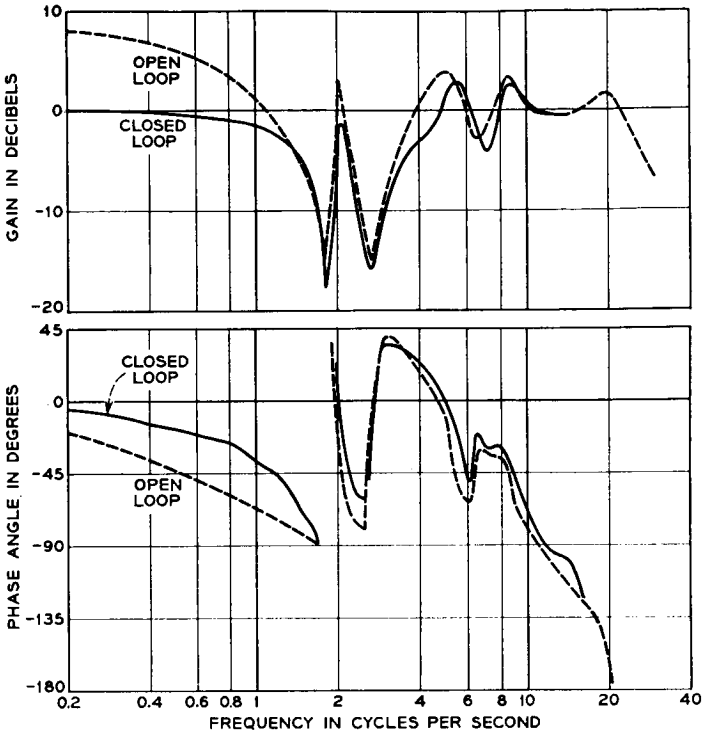

Fig. 10 — Open- and closed-loop frequency response of motor velocity — azimuth.

chanical axes of the antenna structure and compare the measured positions with program-predicted commands. This is the so-called program command mode. The other way is to derive the error signal directly from the 4-kmc beacon signal received from the satellite, using an autotrack technique. This is called the autotrack mode. A third operating mode, the so-called combined mode, operates on a combination of the error signals generated from each of the two methods discussed above.

In order to avoid repetition of the same subject matter, each topic is discussed just once as it is introduced. As a result, the section on the program command mode becomes lengthy, while the other two are relatively short.

A functional diagram of the over-all servo system, showing the interconnections of the various individual units and subsystems, is given in Fig. 11. A brief discussion of the system configuration, responses to test

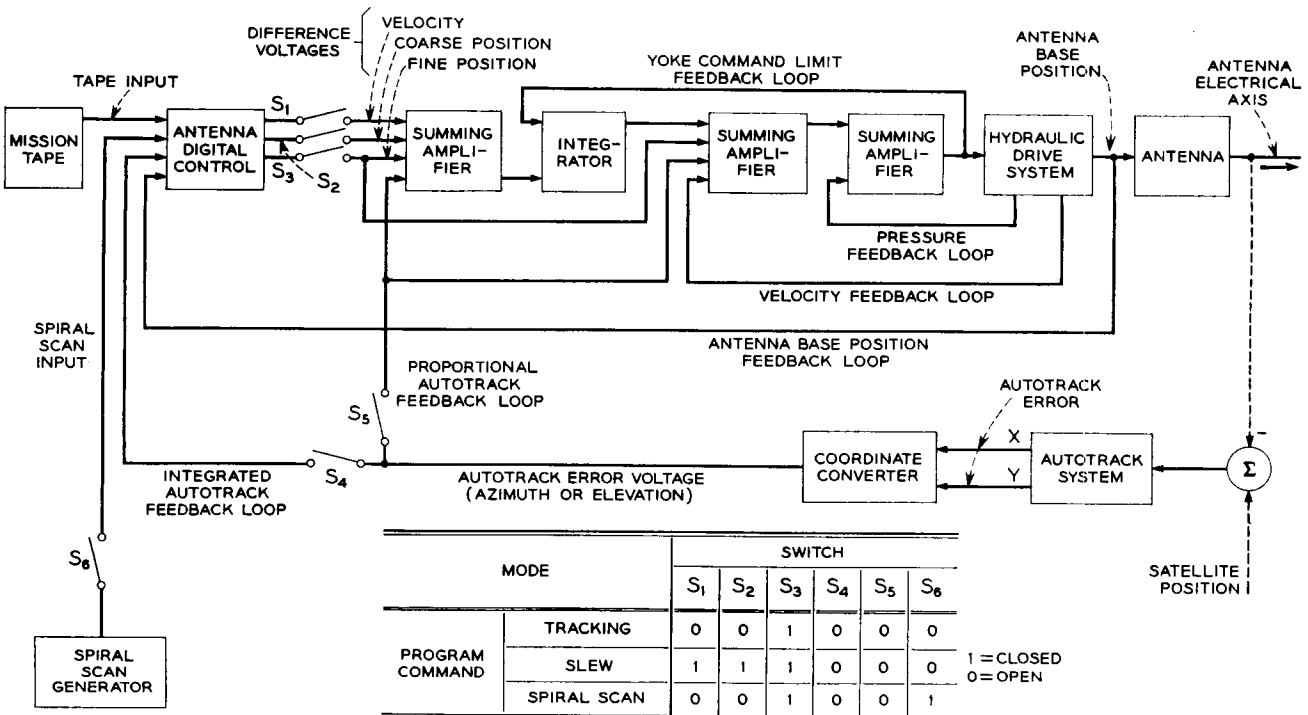

MODE		SWITCH					
		S_1	S_2	S_3	S_4	S_5	S_6
PROGRAM COMMAND	TRACKING	0	0	1	0	0	0
	SLEW	1	1	1	0	0	0
	SPIRAL SCAN	0	0	1	0	0	1
AUTOTRACK		0	0	0	0	1	0
COMBINED		0	0	1	1	1	0

1 = CLOSED
0 = OPEN

Fig. 11 — Over-all functional diagram of the servo system.

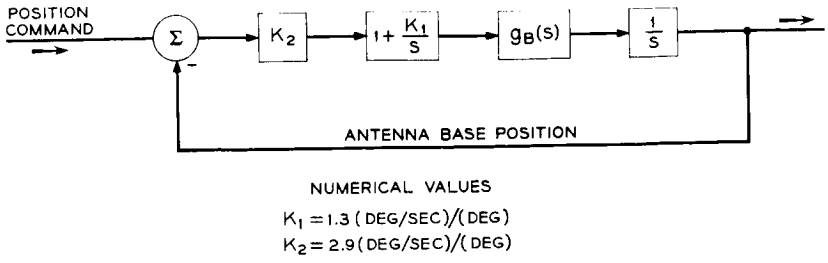

Fig. 12 — Block diagram of servo system in program command mode.

inputs, and the actual tracking performance for each operating mode are presented in the following sections.

4.1 *Program Command Mode*

In the program command mode of operation, the antenna base position is made to follow the program position command provided by the antenna digital control.[3] The block diagram of the system is shown in Fig. 12.

The antenna digital control receives, for a time increment of four seconds, data points from the tape and constructs the position commands. Each data point contains the predicted satellite position, velocity, acceleration, and the time for which it is valid. The position commands are offset to compensate for the differences between the electrical and mechanical axes of the antenna, as measured by star tracking.

The digital unit interpolates between these calibrated data points to provide new pointing information 128 times per second. The antenna digital control also receives the antenna base position information in digital form, compares it with the position command, and decodes the difference to provide a position difference voltage in analog form to the servo drive system.

The position difference voltage is quantized both in amplitude and time. However, the amplitude quantization is so fine (0.00274 degree) and the time quantization is so frequent (128 times per second) that the position difference analog voltage can be treated as a continuous voltage. The position difference voltage saturates at 0.7 degree.

As Fig. 12 shows, the position difference voltage is precompensated by $[1 + (K_1/s)]$, where s is the Laplace transform variable, before it is fed to the drive system. The transfer function $g_B(s)$ relates the antenna base velocity to the drive system input. For all practical purposes, $g_B(s)$ has unity gain in the low frequency region.

The numerical value of K_1 is 1.3°/sec per degree and that of K_2 is 2.9°/sec per degree. The acceleration constant of the system is K_1K_2, or 3.8°/sec² per degree.

The open-loop gain and phase characteristics for the program command mode are shown by Fig. 13. The gain crossover frequency for this

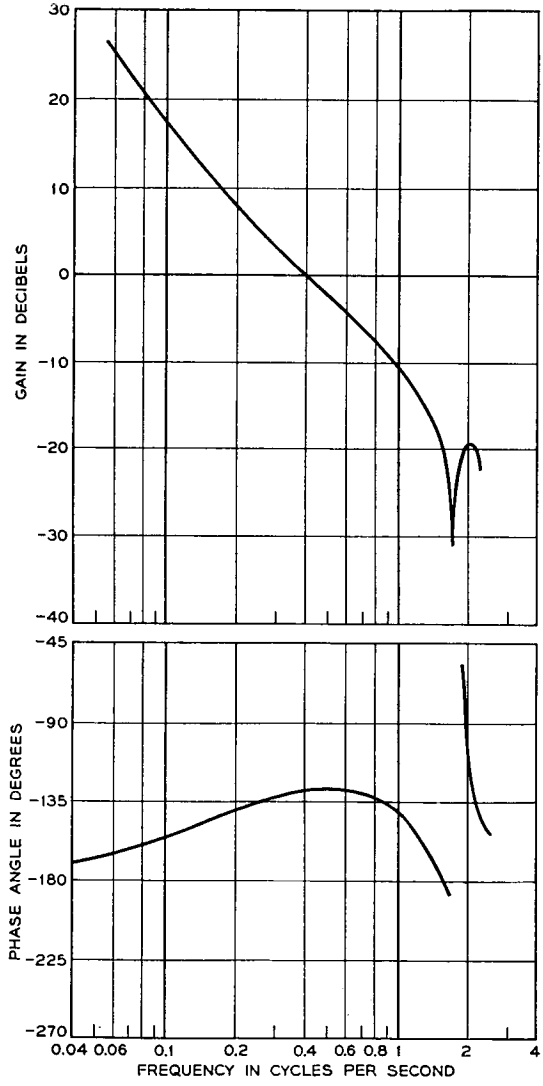

Fig. 13 — Open-loop frequency response of antenna base position — azimuth.

position control loop is 0.4 cps, and the phase margin at gain crossover is 52 degrees. Comparison with the minimum acceptable design objectives illustrated in Fig. 1 shows that the gain versus frequency characteristic realized for the system had the desired shape and that its crossover frequency exceeds the minimum acceptable design objective by 2.5:1. As a direct consequence, it was possible to realize an acceleration constant about 6 times larger than the design objective.

These improvements in loop gain and bandwidth over the minimum acceptable design objectives are due in large part to the increase in fundamental resonant frequency of the antenna structure and drive system from the 0.64 minimum required to the 1.8 cps actually achieved.

The closed-loop frequency response of the system is shown in Fig. 14, and the transient response to a triangular input is presented in Fig. 15. Although these responses are for the azimuth axis only, those for the elevation axis are similar. Input signal magnitudes were chosen to be as

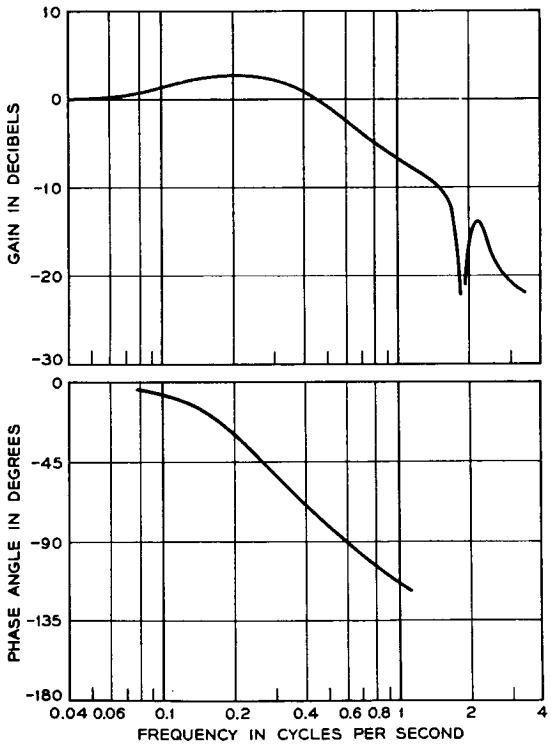

Fig. 14 — Closed-loop frequency response of antenna base position — azimuth.

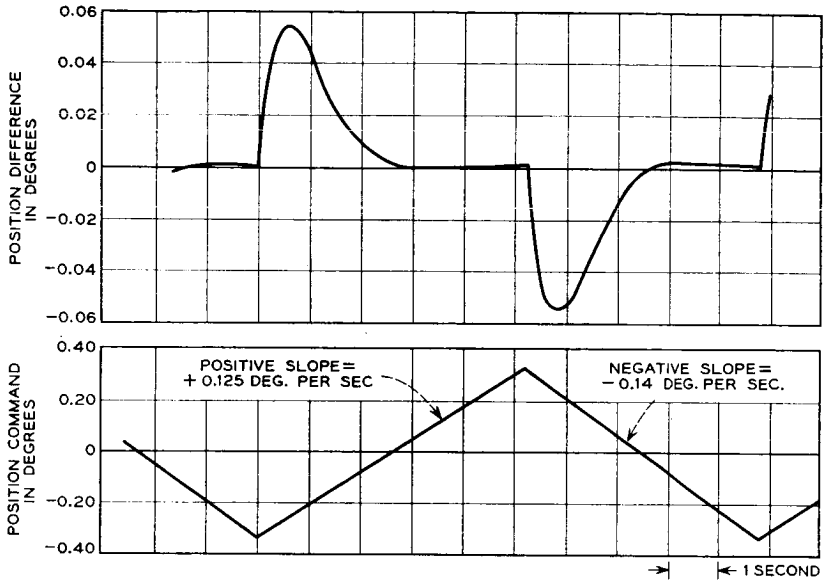

Fig. 15 — Ramp response of program command mode — azimuth.

large as possible but short of saturating the motor torque and velocity. The frequency response curves show that the gain is approximately unity out to 0.4 cps, where the phase lag reaches 60 degrees. Referring to the transient response, the peak position difference in following the position command representing a step velocity change of 0.275 degree per second is 0.055 degree, and the position difference is reduced to zero in less than 3 seconds following each step change in input velocity.

As this is a type 2 servo, the system theoretically follows a constant velocity input with no steady-state error. The acceleration constant for the final system is 3.8°/sec² per degree. This means the position error will not exceed the maximum allowable error of 0.014° for accelerations of less than 0.05°/sec². Since the maximum azimuth acceleration is only 0.026°/sec² for a satellite pass with a maximum velocity of 1.5°/sec, this means that the system can track right up to its maximum slew velocity with an acceleration error of only 0.007°.

The tracking response at low velocities also exceeds the minimum acceptable design objective. The effects of friction have been substantially reduced below the design objectives, since a step in torque of 200,000 ft-lbs applied to the base of the antenna produces a peak position error of less than 0.014°.

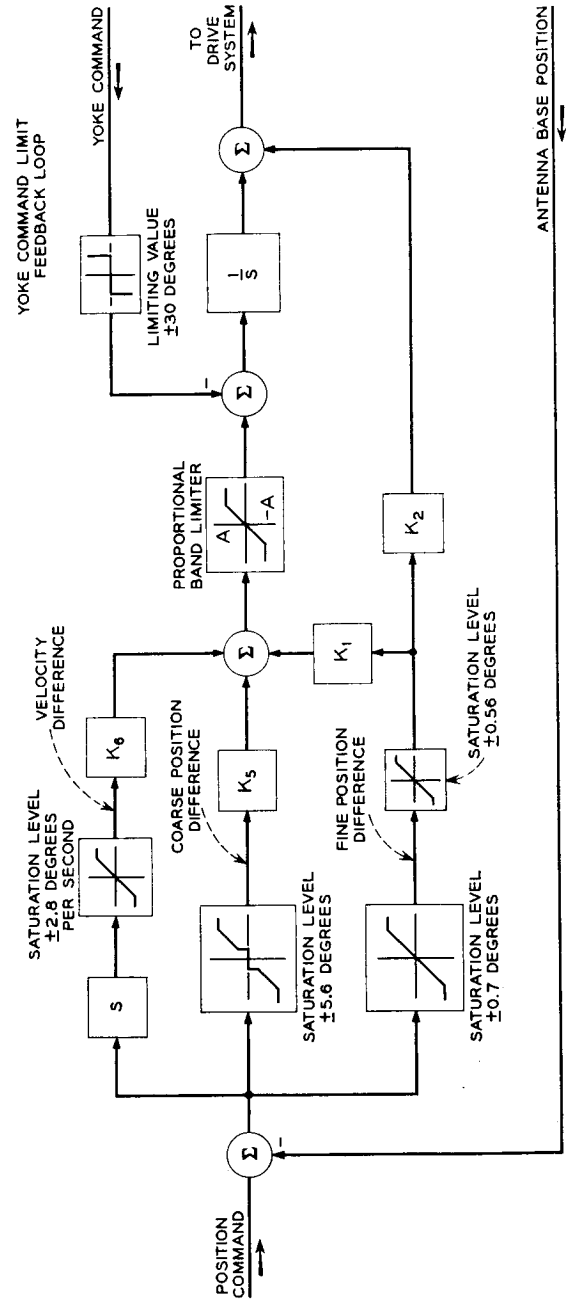

Fig. 16 — Block diagram of the servo system in the program command slew mode.

4.2 *Program Command Slewing*

Program command mode slewing required special attention. Initially, it is necessary to slew the antenna from any arbitrary position to acquire a moving satellite for the start of tracking. The block diagram of the servo system in the program command slew mode shown in Fig. 16 supplements the subsequent discussion.

The tracking servo in the program command mode is actuated by the output of the fine position difference decoder, which produces a proportional difference voltage up to $\pm 0.7°$, but saturates beyond this value. With only this narrow-proportional range the antenna would overshoot several times and suffer rather violent acceleration changes in coming out of slew. These sudden and repeated reversals of drive torque applied to the structure are undesirable because the antenna structure carries both personnel and a large amount of electronic equipment. In order to eliminate this difficulty, the antenna digital control unit also provides a coarse position difference signal with $\pm 5.6°$ proportional range, and a velocity difference signal with 2.8°/sec proportional range. These outputs are both inhibited automatically when the position difference is less than 0.35° in order not to interfere with the normal tracking characteristics of this mode. The coarse and fine position difference signals and the velocity difference signals are combined to form an activating signal for the drive system.

At the start of a slew the antenna is accelerated by the maximum motor torque up to the velocity limit of the drives. This phase takes less than 1.2 seconds in azimuth, and about 0.5 second in elevation. The constant-speed portion of slew takes the major part of the slewing time. A 90-degree slew takes one minute in azimuth, and a little longer in elevation. During the deceleration phase the applied torque is always less than one-third of the maximum in order to limit the amount of energy stored in the compliance of the horn support structure. The position and velocity differences are reduced simultaneously; (see Fig. 17). When the position difference decreases to 0.35° the control system reverts to a tracking mode of operation; at that time the velocity difference is small enough for the tracking servo to terminate the slew without overshoot (see Fig. 18).

4.3 *Spiral Scan*

The spiral scan facility provides a systematic scan that can be used in conjunction with the program command mode of operation to search for a satellite in an increasing spiral about the commanded position. The pitch of the spiral is 0.2 degree per turn, so that successive scans

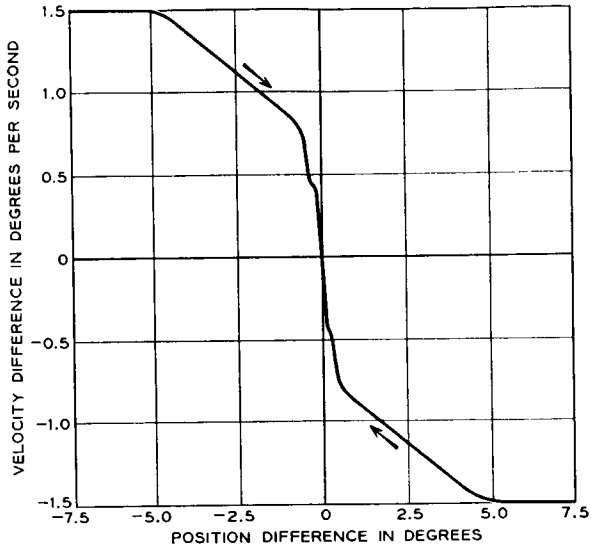

Fig. 17 — Phase plane trajectories of servo system in slew mode — azimuth.

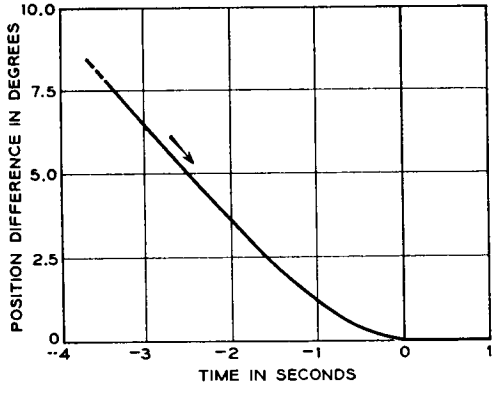

Fig. 18 — Servo system response in slew mode — azimuth.

overlap at the 3-db down point of the antenna beam. In order to scan equal areas in equal times, the angular velocity of the scan is made to decrease as the radius of the scan increases.

Two scanning speeds are provided for fast and slow searching. The fast scan sweeps out a circle with a 1-degree radius in 100 seconds. The slow scan takes 400 seconds to cover the same area. Provisions are made so that the fast scan can be stopped at any time during its scan and a

new slow-speed scan initiated, the center of which is offset from the commanded position by the position of the fast scan at the time the slow scan was initiated.

This spiral scan feature has been used in Telstar tests to search for and acquire the satellite. In a typical test, the high-speed scan was used until indication was received that the antenna had just swept by the satellite. Then the low-speed scan was initiated and the autotrack receiving system was able to achieve phase lock, acquire the satellite, and transfer control to the autotrack mode.

4.4 *Autotrack Mode*

In the autotrack mode, the autotrack error voltages are used to control the antenna position. In other respects the system configuration is essentially the same as that of the program command mode. The block diagram of the system is shown in Fig. 19. The new transfer function $g_E(s)$ relates the antenna electrical axis velocity to the compensated hydraulic drive system input. Here $g_E(s)$ can be considered unity at frequencies below 1 cps.

The value of K_1 is 1.3°/sec per degree and that of K_2 is 1.9°/sec per degree, for both axes. The value of K_2 has been reduced from that used in the program command mode for two reasons. One is to allow for the additional phase lag between the base position and the electrical axis, and the other is to minimize the system transient at the time the autotrack is engaged. The acceleration constant of the system is 2.5°/sec² per degree.

Fig. 20 shows the relation between the autotrack error voltage and corresponding position error for the azimuth axis. The one for elevation is similar. As Fig. 20 shows, for small position errors the slope of the error voltage is very nearly 65 volts per degree. However, the relation is quite nonlinear and the polarity even reverses for angular errors above

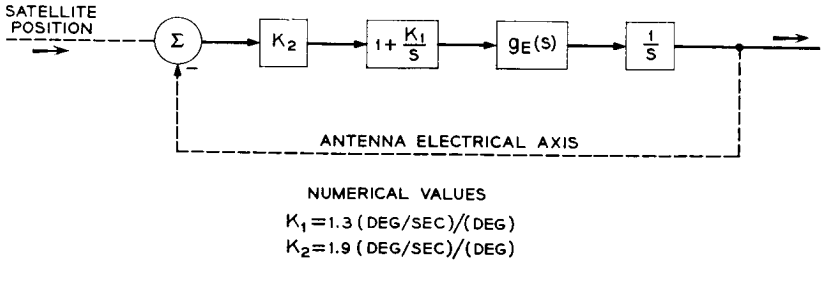

Fig. 19 — Block diagram of servo system in autotrack mode.

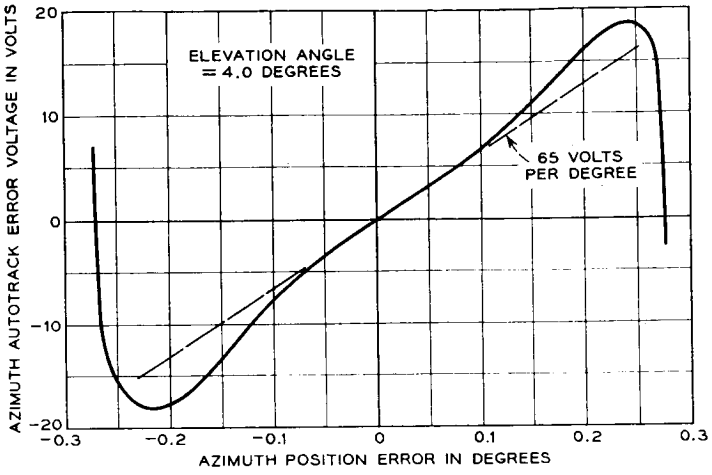

Fig. 20 — Autotrack error voltage versus position error characteristic — azimuth.

0.2 degree. Because of this, the autotrack mode cannot be engaged when the initial pointing error is greater than about 0.15 degree in each axis.

The original autotrack error voltages provided by the autotrack receiving system are in the X and Y coordinate system fixed with respect to the coupler, which does not rotate with the antenna in elevation. These error voltages are converted to elevation and traverse components, and the traverse error voltage is multiplied by the secant of the elevation angle to form the azimuth error voltage.[4]

Fig. 21 shows the transient response characteristics in the autotrack mode when the autotrack loop is closed with an initial error of about 0.1 degree in each axis. These characteristics show that the resulting transients damp out in 4 seconds. Since only the error voltage is available, it is not feasible to measure the open-loop gain and phase characteristics in the autotrack mode.

As in the previous mode, the position error in following a constant velocity is zero, and the position error in following a constant acceleration is proportional to the acceleration. Since the acceleration constant of the system is 2.5 degrees per second squared per degree, this means that the error for the maximum acceleration condition is 0.026 degree per second squared — approximately 0.01 degree.

4.5 *Combined Mode*

The combined mode is a combination of the two previously discussed modes. In this case, the program command and autotrack loops are

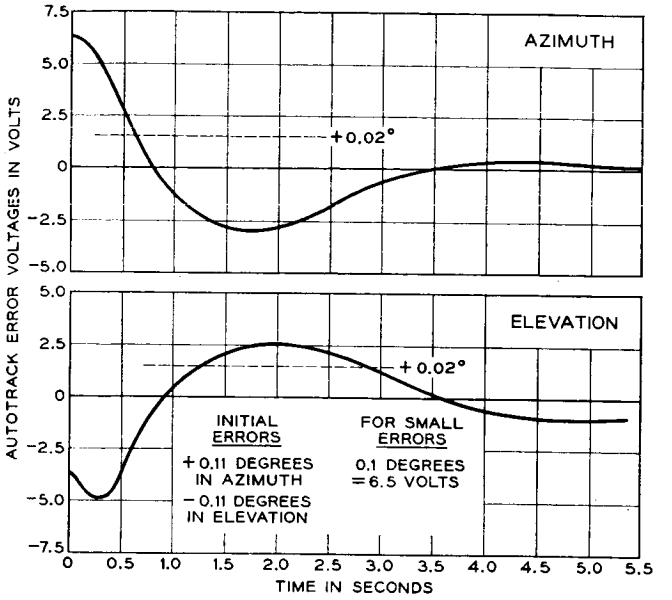

Fig. 21 — Response of servo system in autotrack mode to initial pointing error.

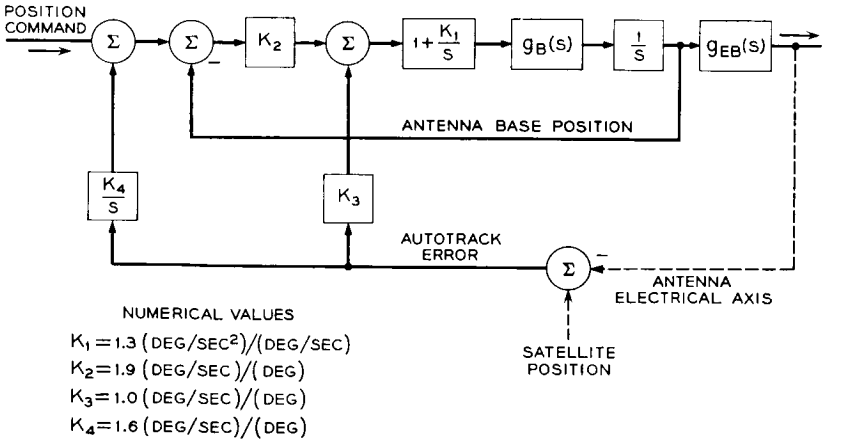

Fig. 22 — Block diagram of servo system in combined mode.

individually closed using the same configurations as before, but with different gains. In addition the autotrack errors are encoded, digitally integrated, and then added to the position command. The configuration is shown on Fig. 22. It is the function of the integrated autotrack error signal to buck out the low-frequency errors in the position command.

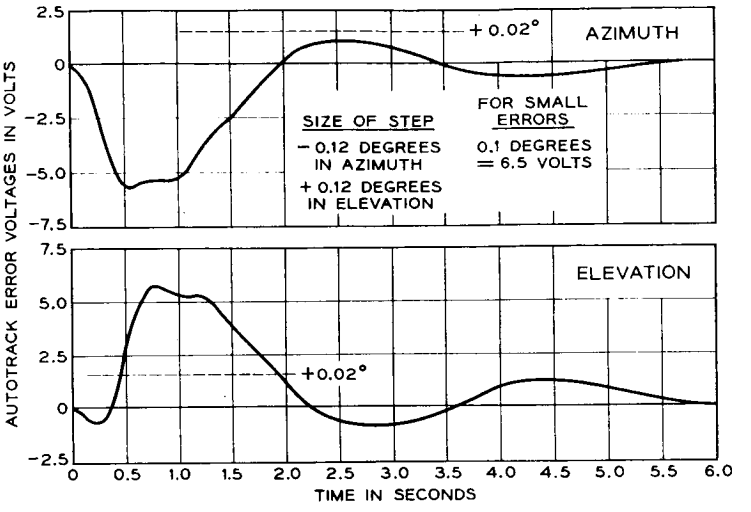

Fig. 23 — Response of servo system in combined mode to step change in program position command.

The relative weights of the program command, proportional autotrack and integrated autotrack loops can be adjusted by changing K_2, K_3, and K_4, respectively. The numerical values of the various gain constants used in the system are 1.3°/sec per degree for K_1, 1.9°/sec per degree for K_2, 1.0°/sec per degree for K_3 and 1.6°/sec per degree for K_4.

In theory, the performance in this combined mode should be comparable to that of the full autotrack mode as long as the errors in the predicted position commands vary slowly as a function of time. However, the higher autotrack loop gain realized in the autotrack mode makes its performance superior to that of the combined mode.

Various step response characteristics for the combined mode are shown in Figs. 23 and 24. Fig. 23 shows the transient response characteristics as measured by the autotrack voltages in response to a step program position command change of 0.12 degree in both axes. The results show that the program position errors are integrated out in less than 6 seconds.

Fig. 24 shows the transients in autotrack error voltages that result from closing the autotrack loop after errors in the program position command had offset the pointing by 0.12 degree both axes. In this case, the pointing errors are reduced to less than 0.01 degree in 5 seconds.

Fig. 25 shows a typical tracking record of the servo system tracking at moderate velocities in the combined mode. Here, the autotrack error

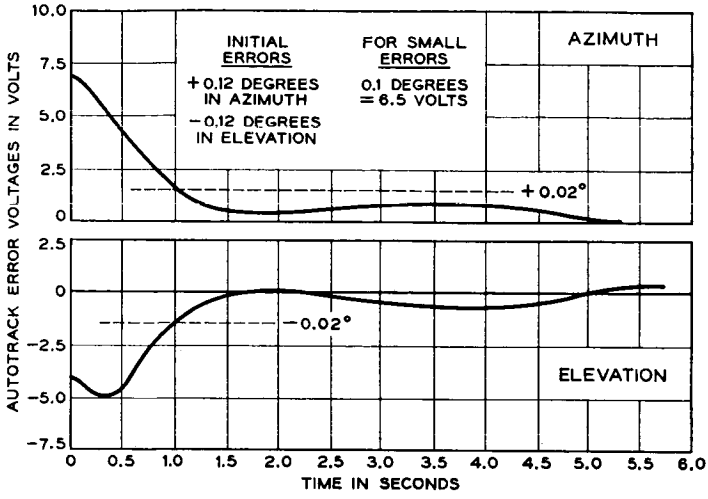

Fig. 24 — Response of servo system in combined mode to initial error in program position command.

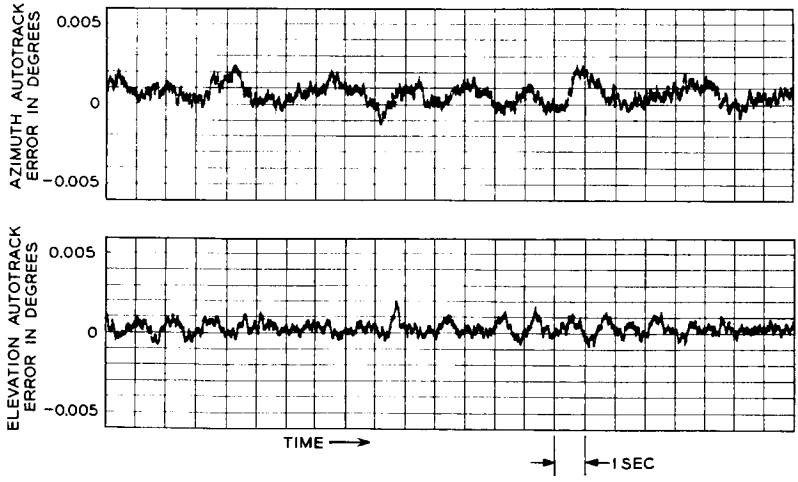

Fig. 25 — Typical tracking record of servo system in combined mode.

voltages are recorded as a function of time. The record shows that the autotrack tracking error voltages in the two axes are less than 0.003 degree. Slowly changing errors in the predicted satellite orbit, distortion of the antenna structure due to gravity, or the effects of quantization

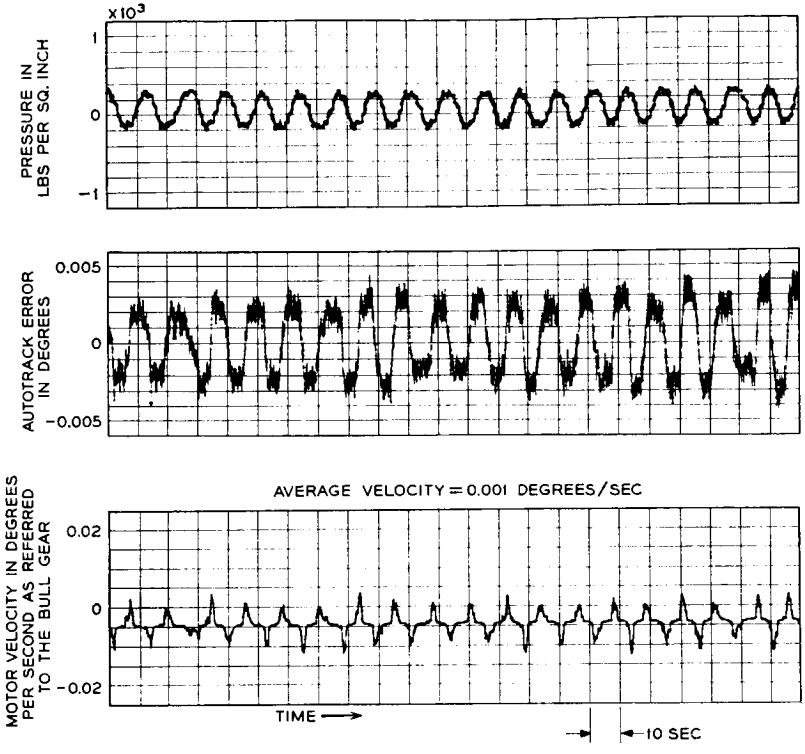

Fig. 26 — Small amplitude hunting in combined mode — azimuth.

in the encoded antenna position do not affect the tracking accuracy in this mode.

The combined mode of operation is subject to a low-amplitude, low-frequency hunting when the tracking velocity in either axis is very low (less than 0.002 degree per second). Hunting about the azimuth axis is shown in Fig. 26. The frequency of the hunting is about 0.17 cps and the corresponding autotrack error can be as large as 0.008 degree.

The hunting phenomenon described above is caused by two factors. One is the extra stage of integration inserted in the autotrack loop to make the autotrack error dominant over the program position command at very low frequencies. The extra integrator makes the combined mode a type 3 servo and, therefore, one which is conditionally stable. The other factor is the reduction in gain of the drive system for small tracking velocities, as discussed previously. This condition is not considered detrimental, because the maximum tracking error is less than 0.008

degree and because the condition disappears when the tracking velocity exceeds 0.002 degree per second.

V. CONCLUSIONS

The design objective called for tracking with a pointing error less than 0.02 degree for all satellite passes where the azimuth velocity is less than 0.5 degree per second. This objective corresponds to tracking a 2500-mile-high satellite up to an elevation angle of 81°.

The relatively high frequency of the first structural resonance and the use of pressure feedback to provide damping of this resonance made it possible to obtain a 2.5:1 increase in bandwidth and a 16-db increase in gain of the position loop over and above the system objectives. The resulting improvement in dynamic performance permits tracking of a 2500-mile satellite up to an elevation angle of 87° rather than the 81° objective.

The servo system has consistently positioned the antenna on the satellite track with an accuracy sufficient to give less than 1-db degradation in antenna gain.

VI. ACKNOWLEDGMENTS

Although it is not possible to give credit to everyone who contributed to the success of this project, the authors wish to acknowledge the work of G. A. Colom, L. Gingerich, W. Lawson, R. Klahn, M. Peak, G. L. Ruzicka, and F. C. Young.

REFERENCES

1. Githens, J. A., Kelly, H. P., Lozier, J. C., and Lundstrom, A. A., Antenna Pointing System: Organization and Performance, B.S.T.J., this issue, p. 1213.
2. Claus, A. J., Blackman, R. B., Halline, E. G., and Ridgway, W. C., III, Orbit Determination and Prediction, and Computer Programs, B.S.T.J., this issue, p. 1357.
3. Githens, J. A., and Peters, T. R., Digital Equipment for the Antenna Pointing System, B.S.T.J., this issue, p. 1223.
4. Cook, J. S., and Lowell, R., The Autotrack System, B.S.T.J., this issue, p. 1283.
5. Dolling, J. C., Blackmore, R. W., Kindermann, W. J., and Woodard, K. B., The Mechanical Design of the Horn-Reflector Antenna and Radome, B.S.T.J., this issue, p. 1137.